Rubber-modified thermosets: Prediction of the particle size distribution of dispersed domains

A. Vázquez, A. J. Rojas, H. E. Adabbo, J. Borrajo and R. J. J. Williams*
Institute of Materials Science and Technology (INTEMA), University of Mar del Plata–National Research Council (CONICET), Juan B. Justo 4302, (7600) Mar del Plata, Argentina
(Received 3 March 1986; revised 28 October 1986; accepted 26 November 1986)

A model predicting the particle size distribution of dispersed domains in rubber-modified thermosets was developed on the basis of a thermodynamic description of the variation of free energy of mixing with conversion and a phase-separation analysis through constitutive equations for nucleation and growth rates. The model includes experimental information illustrating its application to a bisphenol-A diglycidyl ether epoxy resin cured with diaminodiphenylsulphone and containing a carboxyl-terminated acrylonitrile–butadiene random copolymer. Reasonable agreement between predicted and experimental cumulative particle size distributions is shown. Most of the morphological characteristics of the rubber-modified thermoset depend on the location of the reaction extent at which phase separation begins to take place (p_c), with respect to gel conversion (p_{gel}). Increasing the span of the ($p_{gel} - p_c$) range leads to: (a) an increase in the concentration of dispersed particles, (b) an increase in the volume fraction of the dispersed phase, (c) a decrease in the final amount of rubber remaining in the matrix, (d) a decrease in the average concentration of rubber in dispersed particles, and (e) an increase in the concentration of small particles in the overall distribution (a bimodal distribution may result).

(Keywords: rubber-modified; thermoset; toughening; epoxy; compatibility; phase separation; demixing)

Since the pioneering works of McGarry[1] and Soldatos and Burhans[2], it is recognized that brittle thermoset resins may be improved by means of elastomeric inclusions. Rubber-modified thermosets are prepared from a homogeneous solution of an elastomer in a thermosetting resin, which in the course of polymerization precipitates a discrete, randomly dispersed rubbery phase. The two-phase nature of the material greatly improves the crack and impact resistance of the normally brittle matrix. This improvement must be achieved without significant deterioration of bulk properties of the unmodified thermoset, i.e. elastic modulus, glass transition, etc. The increasing importance of these materials is reflected in a recent book giving the first comprehensive coverage of the field[3].

A general description of phase separation was first reported by Visconti and Marchessault[4,5]. A carboxyl-terminated butadiene–acrylonitrile random copolymer (CTBN) was dissolved in a mixture of a cycloaliphatic epoxy resin with an anhydride hardener, in the presence of catalysts. During an initial polymerization period the mixture remained homogeneous; at a certain reaction extent an elastomeric phase precipitated and small domains of a few micrometres in size were detected by transmission electron microscopy (TEM) in thin sections of the solid polymer after staining with OsO_4. The variation in size and shape of the spherical domains was studied as a function of CTBN content by small-angle light scattering. For CTBN concentrations less than 20%, spherical rubber inclusions about 4 μm in size were found by light scattering. Beyond 20%, epoxidic domains of about the same size are present, showing an inversion in the phase separation (as observed by TEM). The morphological changes occurring during polymerization were followed continuously by means of light scattering. It was found that phase separation takes place well before the gelation point, at a time when mobility is still possible. In the commercially important range of 2–15% CTBN, by weight, the system showed a phase separation with a bimodal distribution of rubber particles, some of them being in the desired micrometre range while much smaller particles (~200 Å) were uniformly dispersed in the matrix. At the stage of their appearance, the overall viscosity was much too large, i.e. reaction extent approaching gelation, to allow significant growth.

In a previous work[6] we have developed a model to predict the fraction, composition and average radius of the dispersed phase segregated during a thermoset polymerization (i.e. a rubber-modified epoxy system). However, the size distribution was not predicted. The model was based on a thermodynamic description through a Flory–Huggins equation as well as constitutive equations for nucleation, coalescence and growth rates. Qualitative agreement between model predictions and experimental observations was shown. Thus, the possibility of a phase inversion, the arrest of phase separation at the gel point, the presence of epoxy resin in the dispersed domains, the increase in the volume fraction and average radius of dispersed phase domains with the initial rubber amount, and the appearance of a maximum in the average radius as a function of curing temperature were correctly predicted.

* To whom all correspondence should be addressed

0032-3861/87/071156-09$03.00

The aim of this paper is to present an extension of the previous model enabling the calculation of the particle size distribution of dispersed domains, as well as factors affecting it, and to illustrate model predictions with experimental information for a particular rubber–epoxy system.

PARTICLE SIZE DISTRIBUTION

It is very difficult to state which is the required particle size distribution for toughening purposes. As Siebert[7] pointed out, resolving this question is a problem because changing one parameter in these systems, without affecting other parameters, is difficult. Sultan and McGarry[8] showed the presence of microcavitation around large particles (0.5–5 μm). This mechanism was also discussed by Kinloch *et al.*[9,10], although other toughening possibilities such as microvoid development[11,12], tearing[13,14] and triaxial dilatation[15] of rubber particles have been discussed. On the other hand, it was shown[8] that systems with only small particles (0.01–0.03 μm) exhibit shear banding. Riew *et al.*[16] showed that the generation of a bimodal distribution of rubber particles led to the presence of multiple failure modes.

Although fracture mechanics has not yet given the answer concerning the best particle size distribution for toughening purposes, it is important to identify the variables that may be changed to modify it.

MATERIALS

Rubber-modified epoxy resins were prepared starting from the formulations shown in *Figure 1*. The epoxy resin was a commercial bisphenol-A diglycidyl ether (BADGE), Araldit GY 250 (Ciba-Geigy), with an epoxy content of 5.34 eq kg^{-1} (weight per equivalent $WPE = 187.3$ g eq^{-1}) and $(OH)_0/e_0 = 0.061$. It was cured with 4,4′-diaminodiphenylsulphone (DDS), HT 976 (Ciba-Geigy). The rubber was a random copolymer of butadiene and acrylonitrile (26%), terminated with carboxyl groups (CTBN), Hycar 1300 × 13 (B. F. Goodrich). Its number-average molecular weight was close to 3700 g gmol^{-1} and its density was 0.96 g cm^{-3}.

An adduct was first prepared by reacting the carboxyl groups of the CTBN with an excess of BADGE, in the presence of triphenylphosphine (TPP) as catalyst. Typical formulations (100 parts CTBN, 84 parts BADGE, 0.33 parts TPP) were reacted at 80°C, under a N_2 atmosphere, until the carboxyl groups were reduced to less than 10% of their initial concentration.

The final material was obtained by mixing the adduct with appropriate amounts of CTBN and DDS, in order to get stoichiometry as well as the desired rubber volume fraction. Cure was performed at 120°C for several hours. This temperature leads to a relatively low reaction rate which is convenient for the analysis of the phase-separation process. The reaction was arrested by vitrification at an epoxy conversion close to 0.71 (beyond the gel point)[16].

THERMODYNAMICS OF THE RUBBER–THERMOSET SOLUTION

The initial system may be regarded as a solution of CTBN (component 2) in an epoxy–amine solvent (component 1), i.e. a pseudobinary system. As both components have low molecular weights, an ordinary Flory–Huggins equation may be used to describe the free energy of mixing per unit volume:

$$\Delta G^V = (RT/\bar{V}_{10})[(\phi_1/z_1)\ln\phi_1 + (\phi_2/z_2)\ln\phi_2 + \chi\phi_1\phi_2] \quad (1)$$

where ϕ_1 and ϕ_2 are, respectively, the volume fraction of thermoset (epoxy–amine) and rubber. $\bar{V}_{10}$ is the initial molar volume of the thermoset defined as

$$\bar{V}_{10} = \bar{M}_{n,10}/\rho_1 \quad (2)$$

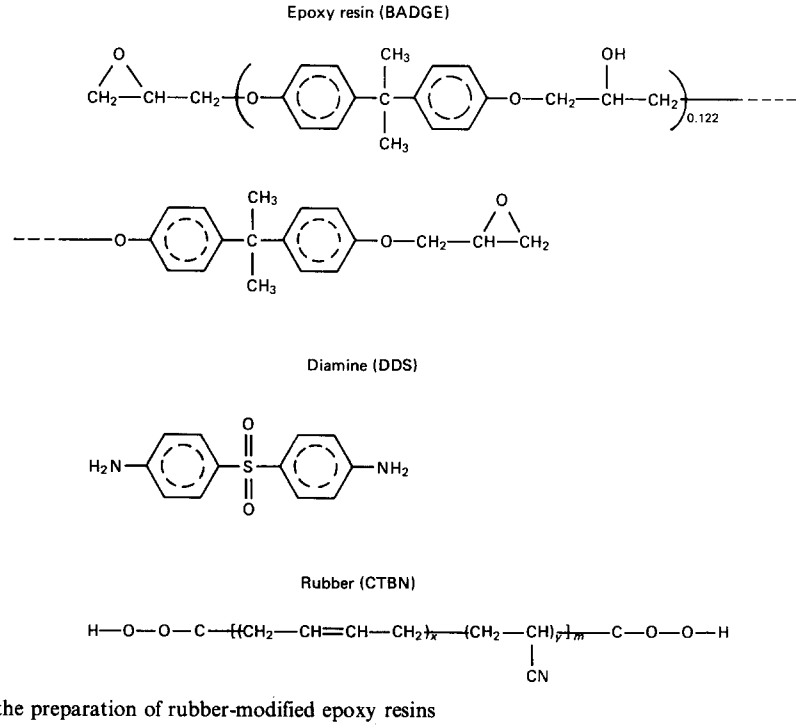

Figure 1 Reagents used in the preparation of rubber-modified epoxy resins

where $\bar{M}_{n,10}$ is the initial number-average molecular weight and ρ_1 is the mass density ($1.2\,g\,cm^{-3}$). By defining

$$\xi = (\text{epoxy equivalents})/(\text{amine equivalents}) = (2B_2)/(4A_4) \quad (3)$$

where B_2 and A_4 represent the number of moles of both monomers, we get

$$\bar{M}_{n,10} = (M_{A_4} + 2\xi M_{B_2})/(1+2\xi) \quad (4)$$

For a stoichiometric mixture, $\xi = 1$ and $\bar{M}_{n,10} = 332.5\,g\,gmol^{-1}$.

If z_1 and z_2 are the ratios of molar volumes of both components with respect to $\bar{V}_{10}$, then

$$z_1 = \bar{V}_1/\bar{V}_{10} \quad (5)$$

$$z_2 = \bar{V}_2/\bar{V}_{10} \quad (6)$$

While z_2 remains constant during the polymerization (for $\xi = 1$, $z_2 = 13.9$), z_1 increases with the thermoset conversion.

The conversions of amine and epoxy equivalents, defined as p_A and p_B, are related through

$$p_A = \xi p_B \quad (7)$$

Then

$$z_1 = \bar{V}_1/\bar{V}_{10} = \bar{M}_{n,1}/\bar{M}_{n,10} = (A_4 + B_2)/(A_4 + B_2 - 4p_A A_4) \quad (8)$$

From equations (3) and (8), we get

$$z_1 = (1+2\xi)/(1+2\xi-4p_A) \quad (9)$$

For a stoichiometric system, $\xi = 1$, $p_A = p_B = p$, and $z_1 = 1/(1-4p/3)$.

It is interesting to point out that as z_1 increases during polymerization, there is a decrease in the absolute value of the entropic contribution to the free energy of mixing (equation (1)). This leads to the demixing of the rubbery phase from a particular reaction extent.

As a first approximation, the Flory–Huggins interaction parameter χ will be considered as a simple function of temperature to be determined experimentally. Its possible variation with composition or conversion will be neglected (notice that as OH groups are generated from the epoxy–amine reaction, the solubility parameter of the thermoset may change leading to variations in the interaction parameter χ).

In order to obtain experimental values of χ, formulations containing different amounts of CTBN (always added as an adduct), in a BADGE/DDS polymer containing an excess of BADGE were prepared. The epoxy excess over the stoichiometric value was such that gelation did not occur even after complete reaction. For the polymerization of an A_4 with an excess of a B_2 (with both functionalities having equal reactivity and without substitution effects), the critical gelation ratio is given by[17]

$$\xi > 3 \quad (10)$$

A value of $\xi = 3.5$ was selected and reaction was carried out to completion at 120°C. From equation (9), $z_1 = 2$ (i.e. the same value obtained for a stoichiometric mixture polymerized to $p = 0.375$).

The cloud points of formulations containing volumetric fractions of rubber ranging from $\phi_2 = 0.12$ to 0.18 were determined by measuring the percentage of transmitted light ($\lambda = 570\,nm$) at different temperatures, each one kept at a constant level for several hours. Both runs made by increasing or decreasing temperatures in several steps gave similar values. *Figure 2* illustrates one such curve for a formulation containing a rubber volume fraction, $\phi_2 = 0.122$. *Figure 3* represents the cloud point temperature as a function of rubber volume fraction, i.e. one of the branches of the binodal curve. It is convenient to point out: (a) that the second branch of the binodal is the one rich in rubber as results from the fact that the minority phase, i.e. the one demixed from the solution, had a lower density than the original solution and went up in the sample tubes; (b) that the behaviour at $\phi_2 < 0.10$ was unexpected, i.e. a maximum appeared, and a careful investigation in this region is under way.

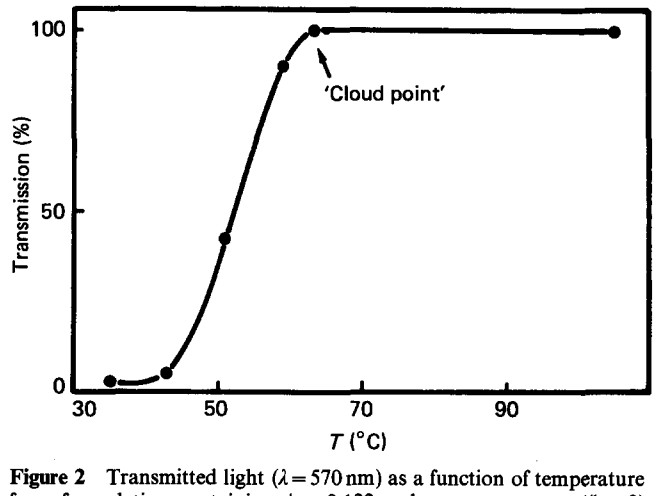

Figure 2 Transmitted light ($\lambda = 570\,nm$) as a function of temperature for a formulation containing $\phi_2 = 0.122$ and an epoxy excess ($\xi_1 = 2$) over the stoichiometric value

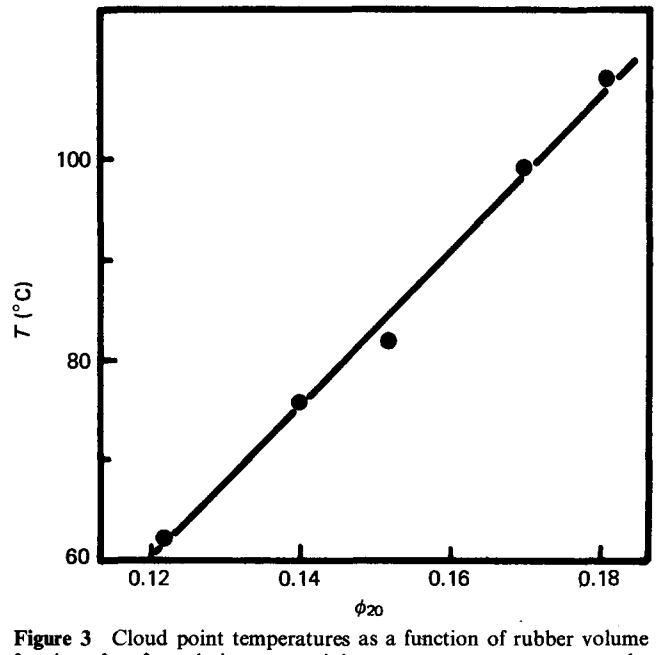

Figure 3 Cloud point temperatures as a function of rubber volume fraction for formulations containing an epoxy excess over the stoichiometric value

Equation (1) may also be written as

$$\Delta G^{v} = (RT/\bar{V}_{10})(\Delta\mu_1\phi_1 + \Delta\mu_2\phi_2) \quad (11)$$

where $\Delta\mu_1$ and $\Delta\mu_2$ are the chemical potentials, per unit volume, of both components:

$$\Delta\mu_1 = (1/z_1)\ln\phi_1 + (1/z_1 - 1/z_2)\phi_2 + \chi\phi_2^2 \quad (12)$$

$$\Delta\mu_2 = (1/z_2)\ln\phi_2 + (1/z_2 - 1/z_1)\phi_1 + \chi\phi_1^2 \quad (13)$$

At equilibrium, i.e. at the cloud point temperature,

$$\Delta\mu_1^{\alpha} = \Delta\mu_1^{\beta} \quad (14)$$

$$\Delta\mu_2^{\alpha} = \Delta\mu_2^{\beta} \quad (15)$$

where α represents the continuous phase (rich in epoxy) and β the dispersed phase (rich in rubber).

As the amount of phase β at the cloud point is negligible, $\phi_2^{\alpha} = \phi_{20}$ and $\phi_1^{\alpha} = 1 - \phi_{20}$. Then, equations (14) and (15) have two unknowns: $\phi_2^{\beta}(\phi_1^{\beta} = 1 - \phi_2^{\beta})$ and χ. By solving the equations by a Newton–Raphson algorithm, the value of χ may be obtained for every ϕ_{20} (associated with a particular temperature, as shown in *Figure 3*).

Figure 4 shows a plot of the interaction parameter χ as a function of $1/T$. The best regression is given by

$$\chi = 0.336 + 69.457/T(\mathrm{K}) \quad (16)$$

Now that we know all the parameters included in the Flory–Huggins equation (equation (1)), the binodal and spinodal curves may be calculated by the usual procedures[6]. For a stoichiometric BADGE/DDS system, at $T = 120°C$, the curves shown in *Figures 5* and *6* result (both represent different regions of the same system).

In the reaction extent vs. rubber volume fraction diagram, tie lines (joining the α and β phases) are horizontal. The stable region (homogeneous solution) is located below the equilibrium curve; the unstable area is located above the spinodal curve; and the metastable region lies between both curves. The inversion point is located at a rubber volume fraction close to $\phi_{20} = 0.26$. For lower rubber amounts, a dispersed phase (β) rich in rubber will be demixed from the continuous phase (α). For example, at $\phi_{20} = 0.122$, the binodal will be reached at a critical reaction extent $p_c = 0.363$. The phase that is demixed at this point has a composition $\phi_2^{\beta} = 0.46$ (*Figure 6*). Thus, although the dispersed phase is richer in rubber than the matrix, significant amounts of the thermoset are present in the dispersed domains.

Once in the metastable region the evolution of the matrix composition, ϕ_{2c}, follows a particular trajectory such as the one depicted in *Figure 5*. Clearly its location will depend on the ratio of the intrinsic rate of phase separation with respect to the polymerization rate. If this ratio is high, i.e. phase separation proceeds very much faster than polymerization, the trajectory will be close the binodal curve (ϕ_{2c} close to ϕ_2^{α}). For low values of the ratio, i.e. polymerization taking place very much faster than phase separation, the trajectory will be a vertical until spinodal demixing takes place.

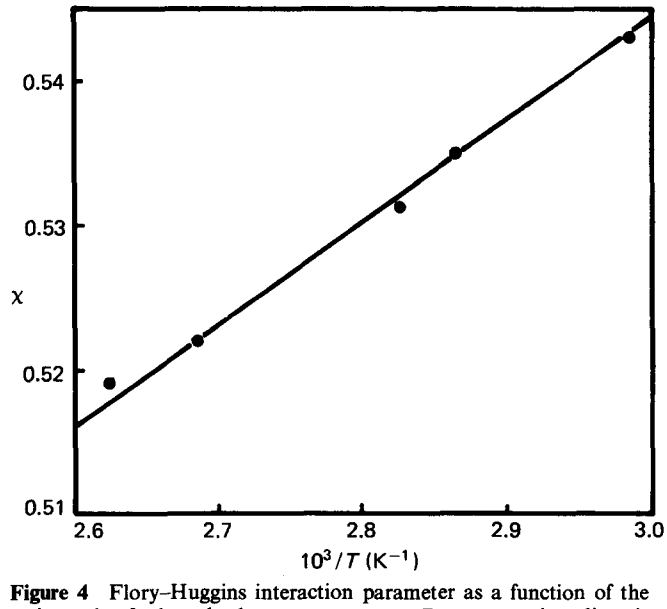

Figure 4 Flory–Huggins interaction parameter as a function of the reciprocal of the absolute temperature. Best regression line is $\chi = 0.336 + 69.457/T(\mathrm{K})$

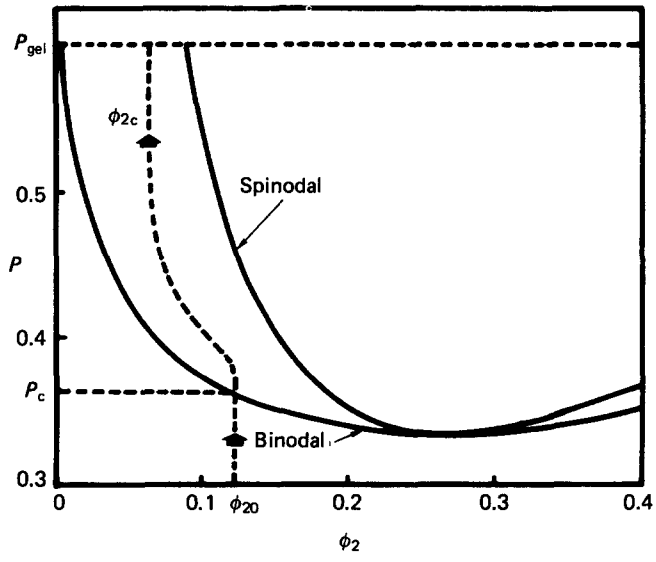

Figure 5 Binodal and spinodal curves for CTBN dissolved in a stoichiometric BADGE/DDS system plotted in a conversion vs. rubber volume fraction diagram, at $T = 120°C$. The dotted trajectory is referred to in the text

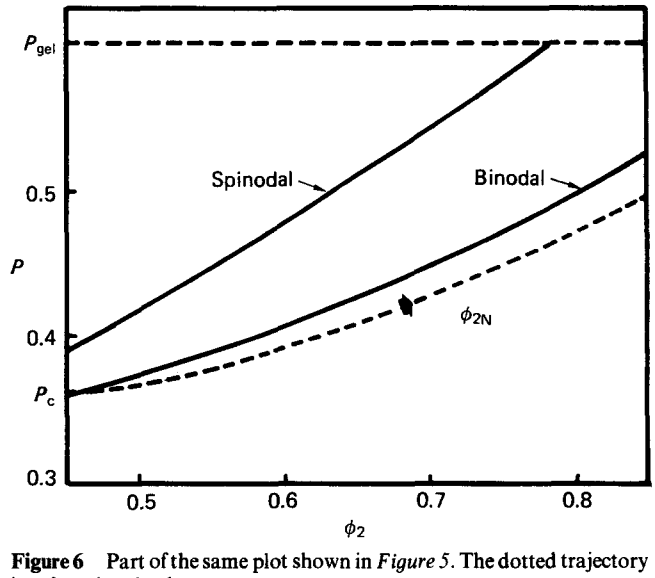

Figure 6 Part of the same plot shown in *Figure 5*. The dotted trajectory is referred to in the text

PHASE SEPARATION

In order to produce a driving potential for phase separation in a homogeneous system it is necessary to enter the metastable region. Let ϕ_{2c} be the actual rubber concentration in the continuous phase at a certain reaction extent. *Figure 7* shows a qualitative plot of the free energy per unit volume at the selected reaction extent. ϕ_2^α and ϕ_2^β are the conjugated points of the binodal curve (equilibrium compositions). The fact that $\phi_{2c} > \phi_2^\alpha$ implies that the system is evolving in the metastable region. The tangent line at ϕ_{2c} gives the virtual free energy per unit volume of any solution segregated from the matrix with composition ϕ_{2c}. The vertical distance between the tangent line at ϕ_{2c} and the free energy curve represents the free energy change per unit volume for the separation of a new phase with any arbitrary composition. For the particular composition ϕ_{2N}, the maximum value of the free energy change per unit volume, ΔG_N, is obtained. Thus ϕ_{2N} represents the actual composition of the segregated phase, and ΔG_N the corresponding free energy change per unit volume. It may be seen that ϕ_{2N} is always greater than ϕ_2^β. A possible trajectory giving the instantaneous composition of the segregated phase, ϕ_{2N}, during polymerization is shown in *Figure 6*.

Most of the experimental evidence regarding the morphology of the dispersed phase in these systems[3] supports the presence of a nucleation–growth mechanism. Moreover, except for very incompatible rubbers which may demix at very low conversions, the possibility of coalescence of dispersed domains is prevented by the large increase of the thermoset viscosity[6].

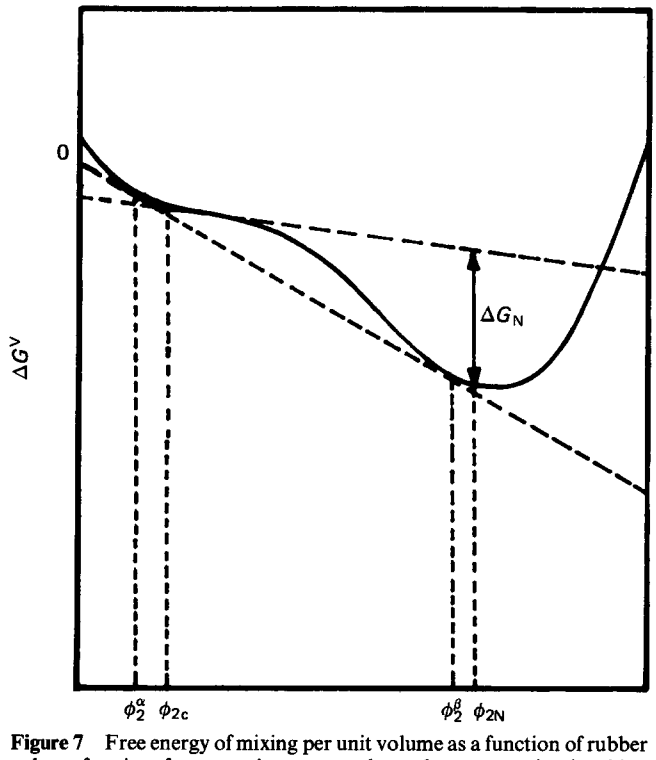

Figure 7 Free energy of mixing per unit volume as a function of rubber volume fraction, for a reaction extent where phase separation is taking place. ϕ_2^α and ϕ_2^β are the conjugated points of the binodal curve, ϕ_{2c} is the actual rubber concentration in the continuous phase, ϕ_{2N} represents the actual rubber concentration of the segregated phase, and ΔG_N the free energy change per unit volume, associated with the phase separation process

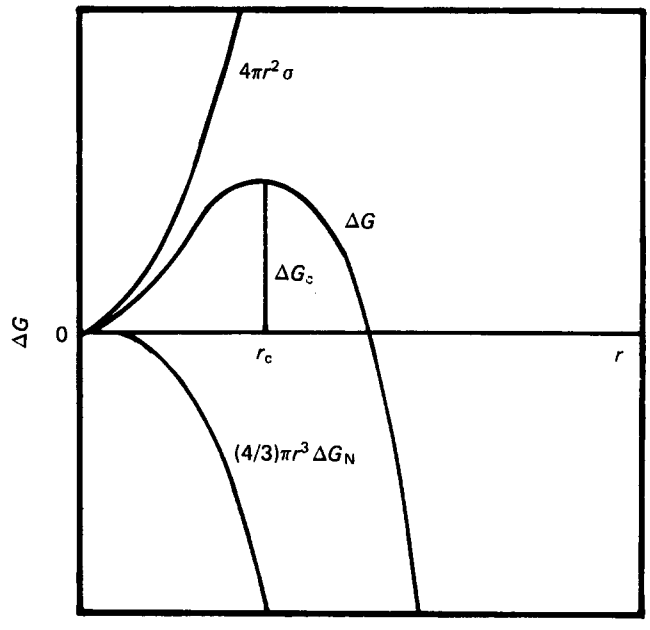

Figure 8 Different contributions to the free energy change associated with the formation of spherical domains

Nucleation rate

The free energy change for the formation of a spherical particle, with composition ϕ_{2N}, is given by

$$\Delta G = (4/3)\pi r^3 \Delta G_N + 4\pi r^2 \sigma \qquad (17)$$

where r is the radius of the spherical domain and σ is the surface tension between both phases. Any elastic strain energy arising from the formation of the new phase is considered negligible.

A plot of equation (17) is shown in *Figure 8*: ΔG reaches a maximum (ΔG_c) for the critical radius, r_c. From equation (17), we obtain

$$r_c = 2\sigma/|\Delta G_N| \qquad (18)$$

$$\Delta G_c = 16\pi\sigma^3/(3|\Delta G_N|^2) \qquad (19)$$

Dispersed domains with a radius $r = r_c$ are called nuclei because their growth decreases the free energy, as shown in *Figure 8*.

The rate of homogeneous nucleation from condensed phases may be written as[18]

$$dP(r_c)/dt = N_0 D \exp(-\Delta G_c/kT) \qquad (20)$$

where $P(r_c)$ is the volumetric concentration of particles with critical radius r_c (nuclei), D is the diffusion coefficient of the rubber in the thermoset, N_0 is an adjustable pre-exponential factor and k is the Boltzmann constant.

In order to calculate the nucleation rate for our particular system it is necessary to estimate values of the surface tension and the diffusion coefficient (notice that N_0 will remain as an unknown parameter which will be adjusted through the experimental determination of the concentration of dispersed phase particles).

Figure 9 shows the surface tension of both epoxy resin and rubber, as a function of temperature, resulting from the capillary rise technique. The surface tension of the rubber–epoxy system, taken as a model of the phase α

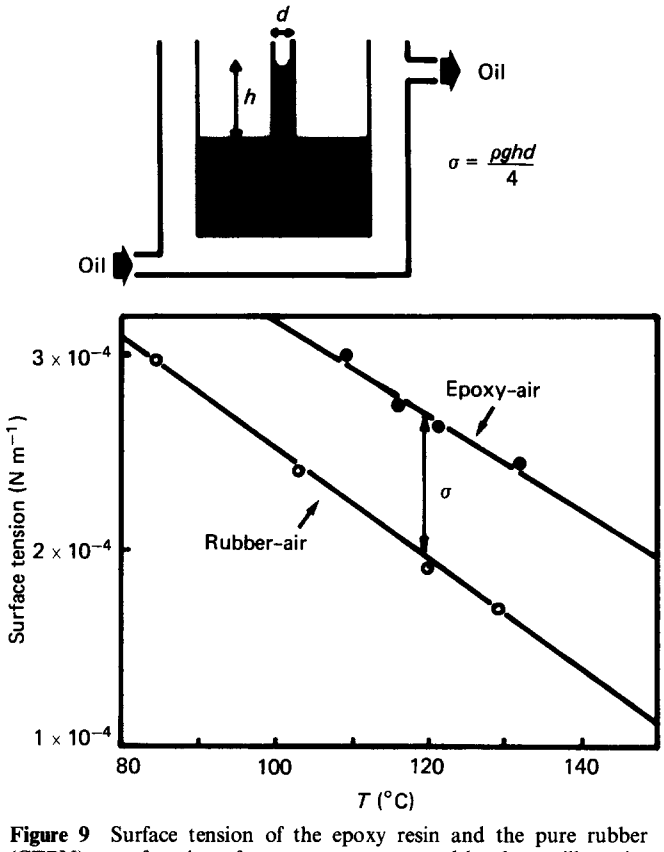

Figure 9 Surface tension of the epoxy resin and the pure rubber (CTBN), as a function of temperature, measured by the capillary rise technique

(composition ϕ_{2c}–phase β (composition σ_{2N}) system, is the difference between both curves as depicted in the figure. As will be shown later, the surface tension has practically no effect on the final size of dispersed domains (it is the growth that plays a significant role). Then, the modelling of phase α as pure epoxy and phase β as pure rubber may be considered satisfactory.

The diffusion coefficient may be estimated by the Stokes–Einstein equation

$$D = D_0 T/\mu(p,T) \tag{21}$$

where μ is the viscosity of the continuous phase, which is a function of both conversion and temperature.

The viscosity of a stoichiometric BADGE/DDS system containing a CTBN amount equal to $\phi_{20}=0.12$ was continuously monitored at 393 K (120°C), using rotational viscometers (both a Brookfield RVT and a Rotovisco RV3 Haake were used). The conversion of epoxy groups was simultaneously monitored by a standard acid titration. A cross-plot of both results gave the curve shown in *Figure 10*. The gel point of the BADGE/DDS system occurs at a conversion $p=0.601$ (for an A_4+B_2 system, $p_{gel}=0.577$; the increase over the ideal value is due to the lesser reactivity of the secondary amine with respect to the primary one)[19]. At the cloud point conversion, p_c, the viscosity is beginning its fast increase, with the consequent decrease in the value of the diffusion coefficient and the nucleation rate.

Although the factor D_0 in equation (21) may be lumped with the adjustable parameter N_0 in equation (20), it is convenient to estimate its value, as D will independently affect the growth rate. The order of magnitude of diffusion coefficients in liquids of water-like viscosity is $10^{-5}\,cm^2\,s^{-1}$. As the initial viscosity of the BADGE/DDS/CTBN system, at 120°C, is close to 10^2 mPa s, i.e. 100 times that of water at room temperature, and taking into account the fact that rubber is a relatively large molecule, the order of magnitude of the diffusion coefficient may be estimated as 10^{-7}–$10^{-8}\,cm^2\,s^{-1}$. Then, the factor was taken as $D_0=10^{-8}$ $(cm^2\,s^{-1})(mPa\,s\,K^{-1})$.

At $p=p_{gel}$, $\mu\to\infty$, $D\to 0$ and nucleation is arrested (in fact, well before gelation the high increase of viscosity leads to very small values for the nucleation rate).

Growth rate

When the system evolves through the metastable region, particle growth occurs because of the driving force $(\phi_{2c}-\phi_2^{\alpha})$, which tries to restore the system to equilibrium conditions. Let us define $dP(r')$ = particles per unit volume that were born at reaction extents between p' and $p'+dp$. At $p=p'$, this set of particles had a radius $r'=r_c(p')$. For $p>p'$, the radius will have grown to a certain value $r'>r_c(p')$. Note, however, that $dP(r')$ is not a function of time.

The growth rate, defined as the increase in volume fraction per unit time, may be assumed to be proportional to the interfacial area per unit volume and the driving force

$$(4\pi/3)dP(r')dr'^3/dt = k_\phi 4\pi r'^2 dP(r')(\phi_{2c}-\phi_2^{\alpha}) \tag{22}$$

k_ϕ is the mass transfer coefficient for a sphere in a stagnant medium, expressed in terms of a volumetric fraction driving force. It is given by[20]

$$k_\phi = D/r' \tag{23}$$

As $D\to 0$ at $p=p_{gel}$, the growth rate is also arrested at gelation.

Structure of the rubber-modified thermoset

The volume fraction of dispersed phase demixed at reaction extents between p and $p+dp$, $dV_D(p)$, includes

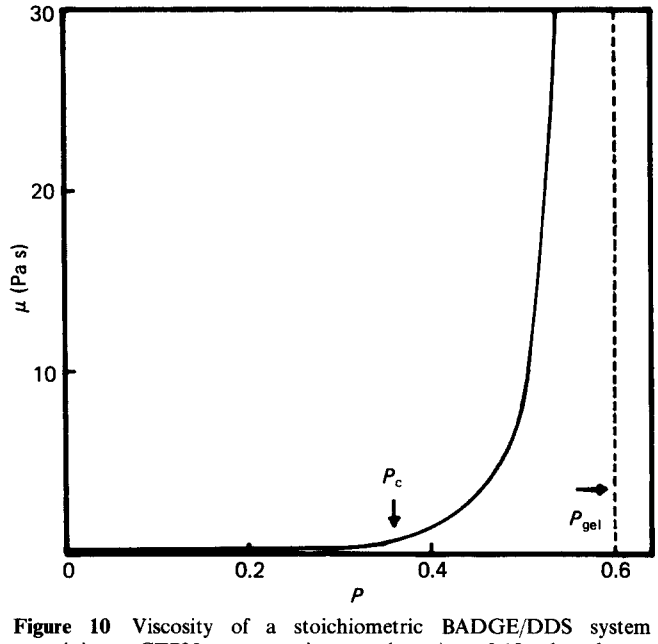

Figure 10 Viscosity of a stoichiometric BADGE/DDS system containing a CTBN concentration equal to $\phi_{20}=0.12$, plotted as a function of the reaction extent of epoxy groups, at 120°C

the new particles appearing at p, plus the volume fraction added to the set of particles born at $p' < p$:

$$dV_D(p) = (4\pi/3)[r_c(p)]^3 dP(r_c) + 4\pi \int_{p'<p} r'^2 dP(r') dr' \quad (24)$$

All this material segregated at reaction extents between p and $p+dp$ has the composition ϕ_{2N} shown in *Figure 7*.

The total concentration of dispersed phase particles per unit volume, at any reaction extent p, is given by

$$P = \int_{p' \leq p} dP(r') \quad (25)$$

A cumulative distribution of particles with radii less than or equal to an arbitrary value r may be defined as

$$P(r) = \int_{\substack{p' \leq p \\ r' \leq r}} dP(r') \quad (26)$$

Then, the size distribution function of particles in the dispersed phase may be calculated as $dP(r)/dr$.

The volume fraction of dispersed phase, at any reaction extent p, is given by

$$V_D = (4\pi/3) \int_{p' \leq p} r'^3 dP(r') \quad (27)$$

A volumetric average diameter of the distribution of dispersed phase particles may be calculated as

$$\bar{D} = (6V_D/\pi P)^{1/3} \quad (28)$$

An average rubber concentration in the dispersed phase may be defined as

$$\bar{\phi}_{2D} = (1/V_D) \int_{p' \leq p} \phi_{2N}(p') dV_D(p') \quad (29)$$

If ϕ_{20} is the initial volume fraction of rubber in the system, the remaining rubber concentration in the continuous phase may be calculated as

$$\phi_{2c} = (\phi_{20} - V_D \bar{\phi}_{2D})/(1 - V_D) \quad (30)$$

RESULTS AND DISCUSSION

Equations (20) and (22) were numerically solved using an Euler method, with the reaction extent p as the independent variable (the p vs. t transformation was made using the experimental curve determined at 120°C). Equations (24) to (27) and (29) were solved by using increments instead of differentials and summations instead of integrals. Convergence was analysed by varying the selected increment Δp.

An overall check of the model was made by analysing fracture surfaces of samples cured at 120°C by scanning electron microscopy (SEM). The number fraction of particles in a particular range of diameters was counted in magnified photographs containing a statistical number of dispersed phase particles (the resolution was adequate for diameters greater than 0.5 μm). For example, for a stoichiometric BADGE/DDS sample containing a CTBN amount equal to $\phi_{20} = 0.122$ and cured for several hours at 120°C, SEM analysis led to $P = 8.2 \times 10^9$ part/cm^3 (total concentration of particles), $V_D = 0.093$ (volume fraction of dispersed phase). The value of P predicted by the model could be adjusted to the experimental value by taking $N_0 = 1.54 \times 10^{16}$ cm^{-5}. The volumetric fraction of dispersed phase predicted by the model is $V_D = 0.096$, in very good agreement with the experimental value. The comparison between predicted and experimental cumulative particle size distributions is shown in *Figure 11*. Taking into account the hypotheses and estimations which were necessary to build up the model, the agreement between both curves may be considered satisfactory.

The model does also predict the trajectories of ϕ_{2c} and ϕ_{2N} which are plotted in *Figures 5* and *6*. The amount of rubber remaining in the continuous phase, ϕ_{2c}, does not change significantly after a reaction extent close to $p = 0.5$. This agrees with the rapid increase in viscosity in this conversion range (*Figure 10*). At gelation, $\phi_{2c} = 0.0643$ (i.e. only 47% of the initial rubber was segregated from the matrix). At this point, the average rubber concentration in the dispersed domains is $\bar{\phi}_{2D} = 0.665$. As may be seen from *Figure 6*, particles born at high conversions (in the separation range) will be richer in rubber than older particles. Moreover, if a possible redistribution of components in a dispersed phase particle is neglected, its nucleus may be pictured as richer in the thermosetting matrix than its periphery. It is remarkable that, working with similar systems, Shah *et al.*[21] showed the presence of a large fraction of unstained epoxy

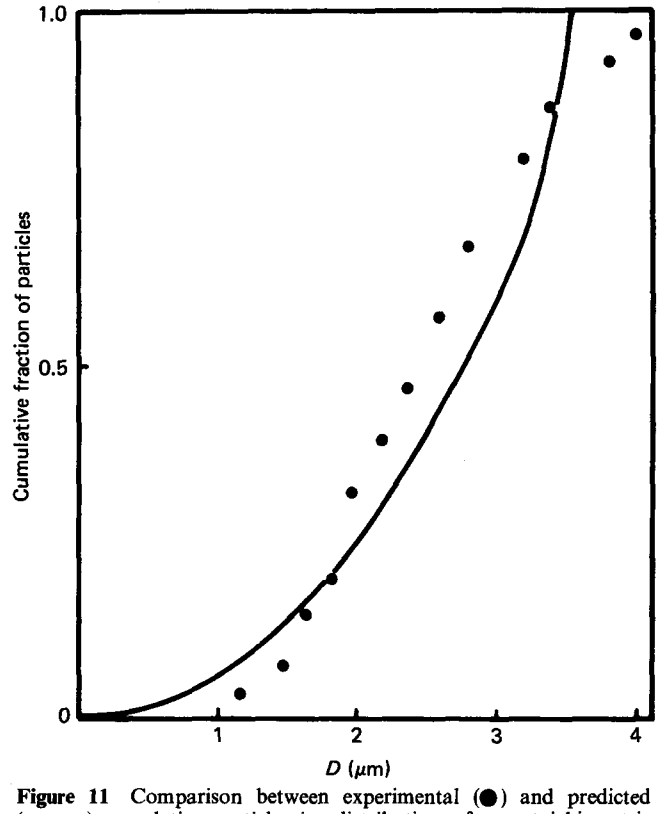

Figure 11 Comparison between experimental (●) and predicted (———) cumulative particle size distributions, for a stoichiometric BADGE/DDS sample containing a rubber concentration $\phi_{20} = 0.122$, and cured at 120°C

domains within the rubbery phase, as well as the segregation of rubber in the interfacial region.

Figure 12 shows a representation of nucleation and growth rates (equations (20) and (22)), in arbitrary units, as a function of reaction extent. Both processes of phase separation are significant in the same conversion range. However, this is not necessarily true for every system. For example, when the rubber is replaced by a CTBN containing less acrylonitrile, its compatibility with the epoxy–diamine resin decreases and phase separation takes place early during the polymerization. *Figure 13* shows the resulting nucleation and growth rates, in arbitrary units. As phase separation occurs in a low-viscosity medium, the trajectory of ϕ_{2c} in the metastable region approaches very rapidly the binodal curve, due to the high value of the diffusion coefficient. The small driving force $(\phi_{2c}-\phi_2^{\alpha})$ provokes a significant decrease in the growth rate while nucleation is still active. The overall result is the generation of a bimodal distribution of diameters, as is shown in *Figure 14*. The simulation was carried out using the same parameters leading to the curves of *Figure 13*. Very early during the phase separation process a sharp distribution of medium-sized particles is obtained (curve A). As polymerization goes on, large particles show a rapid growth while small particles appear as a tail towards low radii in the broadened distribution (curve B). As gelation is approached the growth of large particles is severely retarded while the concentration of small particles increases significantly. This is due to the fact that the growth rate is inversely proportional to the size of the dispersed domains, through the dependence of the mass transfer coefficient.

In general, model simulations showed that decreasing compatibility of the rubber with the thermoset, i.e. increasing the value of χ, leads to: (a) an increase in the concentration of dispersed phase particles, (b) an increase in the volume fraction of the dispersed phase, (c) a decrease in the final amount of rubber remaining in the matrix, (d) a decrease in the average concentration of rubber in dispersed particles, and (e) an increase in the concentration of small particles in the overall distribution. This is all a consequence of the fact that phase separation takes place well before p_{gel}, in a low-viscosity medium.

Regarding the influence of surface tension, simulations varying the experimental value of σ from 2σ to $\sigma/2$ showed no significant changes in the final particle size distribution (a 3 to 4% increase in V_D and P was observed when decreasing the surface tension from 2σ to $\sigma/2$). This is due to the fact that once in the metastable region, the factor $\Delta G_c/kT$ in equation (20) is so small that it has no significant influence on the nucleation rate. On the other

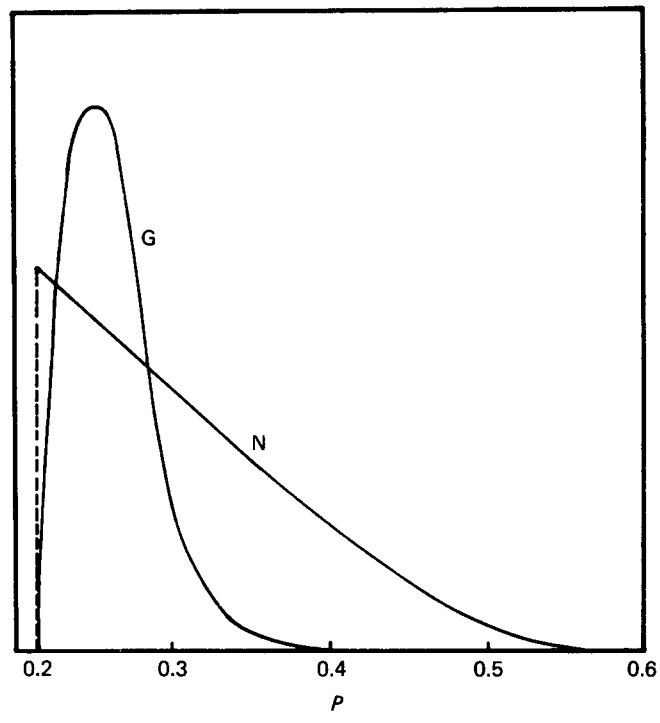

Figure 13 Nucleation (N) and growth (G) rates, in arbitrary units, as a function of reaction extent (less compatible CTBN than the one described in *Figure 1*)

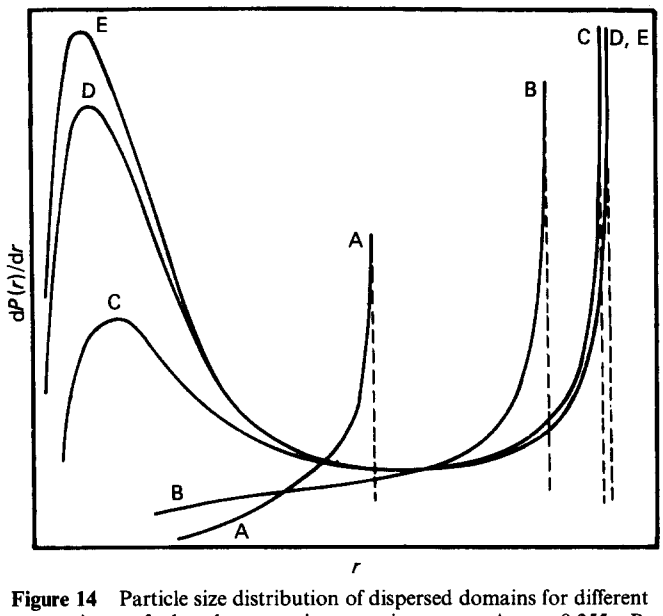

Figure 14 Particle size distribution of dispersed domains for different conversions of the thermosetting matrix: curve A, $p=0.255$; B, $p=0.295$; C, $p=0.395$; D, $p=0.495$; E, $p=0.553$

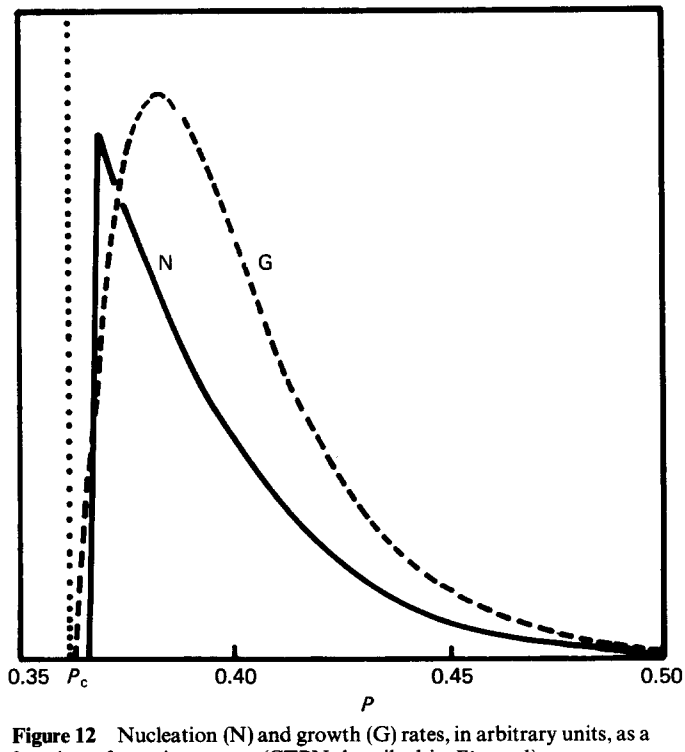

Figure 12 Nucleation (N) and growth (G) rates, in arbitrary units, as a function of reaction extent (CTBN described in *Figure 1*)

hand, although r_c is directly proportional to σ (equation (18)), the fact that the mass transfer coefficient is inversely proportional to the size of particles makes the final size almost independent of the critical radius, r_c.

CONCLUSIONS

A model predicting the particle size distribution of dispersed domains in rubber-modified thermosets was developed on the basis of a thermodynamic description of the variation of free energy of mixing with conversion and a phase separation analysis through constitutive equations for nucleation and growth rates. This model not only improves our first theoretical analysis[6], but also includes experimental information illustrating the application of the theoretical frame to a particular system. A preliminary comparison of predicted and experimental cumulative particle size distributions gave reasonable agreement.

The reliability of the model rests on the fact that it includes a complete framework based on thermodynamic and kinetic equations describing the process of phase separation. This has to be compared with other approaches which are either qualitative or mainly based on the variation of a single parameter, like χ, throughout the polymerization. Obviously, there is still a great need for experimental information to improve our present knowledge. Particularly important is the dependence of the Flory–Huggins interaction parameter on rubber composition, the presence or absence of an adduct, the stoichiometric ratio of the matrix components, the rubber amount and temperature. Also, the determination of possible changes in viscosity and polymerization kinetics with rubber concentration, as well as the measurement of the diffusion coefficient, need a careful experimental study. On the other hand, the small significance of surface tension on final morphology makes it unnecessary to improve its experimental characterization (i.e. at least in our present state of knowledge).

Most of the morphological characteristics of the rubber-modified thermoset depend on the location of the reaction extent (p_c) at which phase separation begins to take place with respct to gel conversion (p_{gel}). If p_c is very close to p_{gel} the low values of diffusion coefficient (high viscosities) will prevent significant phase separation. If p_c has a very low value, the appearance of particles of a low-density rubbery phase in a medium of very low viscosity may lead to a significant coalescence and undesired macroscopic phase separation. The desired discrete, randomly dispersed rubbery phase is obtained by placing p_c in a suitable operating range. This may be achieved by varying the rubber nature (i.e. increasing the acrylonitrile content of a CTBN will improve compatibility and increase p_c) or by changing the location of p_{gel} with respect to p_c (i.e. by adding a chain extender). Once placed in the suitable operating region, increasing the span of the $p_{gel}-p_c$ range provokes: (a) an increase in the concentration of dispersed phase particles, (b) an increase in the volume fraction of the dispersed phase, (c) a decrease in the final amount of rubber remaining in the matrix, (d) a decrease in the average concentration of rubber in dispersed particles, and (e) an increase in the concentration of small particles in the overall distribution (a bimodal distribution may result).

REFERENCES

1 McGarry, F. J. AIAA/ASME 10th Structures, Structural Dynamics and Materials Conf., New Orleans, April 1969
2 Soldatos, A. C. and Burhans, A. S. in Adv. Chem. Ser., No. 99, American Chemical Society, Washington DC, 1971, p. 531
3 Riew, C. K. and Gillham, J. K. (Eds.), Adv. Chem. Ser., No. 208, American Chemical Society, Washington DC, 1984
4 Visconti, S. and Marchessault, R. H. *Polym. Prepr. (Am. Chem. Soc.)* 1974, **15**, 66
5 Visconti, S. and Marchessault, R. H. *Macromolecules* 1974, **7**, 913
6 Williams, R. J. J., Borrajo, J., Adabbo, H. E. and Rojas, A. J. in ref. 3, p. 195
7 Siebert, A. R. in ref. 3, p. 179
8 Sultan, J. N. and McGarry, F. J. *Polym. Eng. Sci.* 1973, **13**, 29
9 Kinloch, A. J., Shaw, S. J., Tod, A. D. and Hunston, D. L. *Polymer* 1983, **24**, 1341
10 Kinloch, A. J., Shaw, S. J. and Hunston, D. L. *Polymer* 1983, **24**, 1355
11 Rowe, E. H. and Riew, C. K. *Plast. Eng.* March 1975, 45
12 Manzione, L. T., Gillham, J. K. and McPherson, C. A. *J. Appl. Polym. Sci.* 1981, **26**, 907
13 Kunz-Douglass, S., Beaumont, P. W. R. and Ashby, M. F. *J. Mater. Sci.* 1980, **15**, 1109
14 Sayre, J. A., Kunz, S. C. and Assink, R. A. in ref. 3, p. 215
15 Bascom, W. D., Cottington, R. L., Jones, R. L. and Peyser, P. *J. Appl. Polym. Sci.* 1975, **19**, 2545
16 Riccardi, C. C. and Williams, R. J. J. *J. Appl. Polym. Sci.* 1986, **32**, 3445
17 Dušek, K., Ilavský, M. and Luňák, S. *J. Polym. Sci., Polym. Symp.* 1976, **53**, 29
18 Doremus, R. H. 'Rates of Phase Transformations', Academic Press, Orlando, 1985, p. 65
19 Riccardi, C. C. and Williams, R. J. J. *Polymer* 1986, **27**, 913
20 Sherwood, T. K., Pigford, R. L. and Wilke, Ch. R. 'Mass Transfer', McGraw-Hill, New York, 1975, p. 215
21 Shah, D. N., Attalla, G., Manson, J. A., Connelly, G. M. and Hertzberg, R. W. in ref. 3, p. 117